

## SINUSOIDAL RIBLETS FOR TURBULENT DRAG REDUCTION

S. Cipelli

Institute of Fluid Mechanics, Karlsruhe Institute of Technology, 76131 Karlsruhe, Germany

**M. Quadrio, F. Gattere**

Department of Aerospace Science and Technologies, Politecnico di Milano, 20156 Milan, Italy

**A. Chiarini**

Complex Fluids and Flows Unit, Okinawa Institute of Science and Technology, 904-0495 Okinawa, Japan

**P. Luchini**

Dipartimento di Ingegneria Industriale, Università di Salerno, 84084 Fisciano, Italy

**D. Gatti**

Institute of Fluid Mechanics, Karlsruhe Institute of Technology, 76131 Karlsruhe, Germany

### MOTIVATION

Drag reduction strategies can be classified into two main categories: active and passive. Active techniques typically involve wall movements, either in the spanwise or wall-normal direction, which can achieve significant drag reduction, up to 50% at low Reynolds numbers. However, their industrial application is constrained by substantial power consumption required for wall movement, and more critically, by the technical challenges associated with the physical implementation of the control mechanisms. In contrast, passive techniques, although offering smaller gains in terms of friction reduction, require only modifications to the wall geometry, making them easier to integrate into the aeronautical industry.

This work specifically focuses on riblets, a groovy type of surface geometry belonging to the passive category. Riblets typically achieve a friction drag reduction of 5 ÷ 10% compared to a smooth surface. The underlying physical mechanism for drag reduction with riblets is well understood and can be attributed to a viscous differential effect of the wall on parallel and cross-flow, resulting in a difference between two virtual origins [5]  $\Delta h = h_{\parallel} - h_{\perp}$ , known as the parallel ( $h_{\parallel}$ ) and perpendicular ( $h_{\perp}$ ) protrusion heights. These quantities depend solely on the cross-section shape, as they are always non-dimensionalized with the square root of the groove cross-section area  $l_g$ . The two virtual origins indicate the position of a flat wall capable of producing the same average velocity profiles in the two directions; when the parallel origin is below the perpendicular one, the wall geometry impedes the cross flow more than the longitudinal flow, leading to drag reduction. In turbulent flows, this mechanism fully describes riblet behavior in the viscous regime, where riblets are extremely small, as the  $Re_{\tau}$ -independent roughness function  $\Delta U^+$ , used to quantify drag, is given by  $\Delta U^+ = h_{\perp}^+ - h_{\parallel}^+$  [4]. For riblets of increasing dimensions, [2] showed that the concept of protrusion heights for parallel and transverse flow must be generalized to virtual origins for streamwise ( $l_V^+$ ) and turbulent ( $l_T^+$ ) flows, as drag reduction is generally quantified as  $\Delta U^+ = l_T^+ - l_V^+$ . While the virtual origin for mean flow ( $l_V^+$ ) can always be related to the parallel protrusion height ( $h_{\parallel}^+$ ), the origin for turbulence is a priori unknown and aligns with that of transverse flow only for a limited range of small  $l_g^+$  values, necessitating evaluation

through numerical or physical experiments for larger riblets. For straight riblets, following the observations from [1] regarding the position of maximum drag reduction occurring at approximately  $l_g^+ = 11$ , it is theoretically possible to derive a universal roughness function by accounting for  $\Delta h$ . This implies that viscous calculations aimed at estimating the protrusion heights should be sufficient to approximately characterize the drag reduction curve of a given geometry.

The aim of this work, however, is to test riblets with crests whose spanwise position varies sinusoidally along the longitudinal direction. The idea is to induce spanwise motions in the near-wall flow that mimic those typical of active control techniques, such as spanwise forcing [6]. By doing so, we aim to combine the virtual origin effect characteristic of straight riblets with the drag-reducing benefits of spanwise forcing techniques, exploring a potential enhancement of the performance of straight riblets.

### METHOD

The described geometries are investigated through Direct Numerical Simulations (DNS) in a periodic channel with dimensions of  $(7.5 \delta, 3.75 \delta, 2 \delta)$  in the streamwise, spanwise, and wall-normal directions, respectively, being  $\delta$  the channel half height. The spatial discretization employs second-order finite differences, and the timestep is advanced through a third-order Runge-Kutta scheme. The geometry is represented using an immersed boundary method (IBM). Riblets are present on both walls, and the friction Reynolds number is  $Re_{\tau} = 200$ . Statistics are averaged over 400  $t \delta / u_{\tau}$  time units.

Typically, extremely fine grid spacings are required near the riblet tips to ensure proper flow discretization. However, in this study, we use a uniform grid in the near-wall region where the minimum grid spacing never falls below 0.5 plus-units. This is achievable due to the correction of the IBM with local Stokes and Laplace solutions near the edges. This method, introduced by [3] and previously presented at EDRFCM 2022, allows for the simulation of full channel flows with riblets on a smooth-wall-like grid, maintaining the computational cost around 40 thousand CPU-hours for most configurations.

The simulated geometries include triangular riblets with a

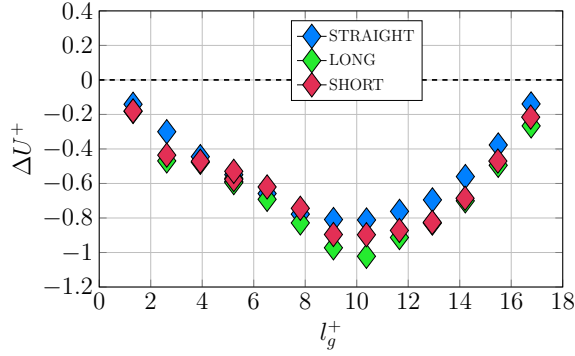


Figure 1: A summary of the  $\Delta U^+$  values obtained for all simulations as a function of the riblets size  $l_g^+$ . The three labels indicate the straight riblets configuration and the two sinusoidal configurations, namely "LONG" and "SHORT".

$60^\circ$  tip angle spanning the entire drag-reducing regime, from  $l_g^+ \approx 1.5$  to  $l_g^+ \approx 16.5$ . We present results for both straight and sinusoidal riblets, where the sinusoidal waves are defined by two additional parameters: the wavelength  $\lambda_x^+$  and the maximum inclination with respect to the x-direction  $\beta_{max}$ . The simulated sinusoidal geometries are characterized by  $(\lambda_x^+, \beta_{max}) = (1500, 2^\circ)$  and  $(250, 12^\circ)$ , labeled as "LONG" and "SHORT" due to their different wavelengths. We calculate  $l_T^+$  by overlapping the ribbed and smooth wall Reynolds shear stress profiles in the near-wall region, considering the total shear stress at the turbulence origin in the evaluation of  $u_\tau$ . Then, all mean velocity profiles are shifted in the wall-normal direction to share the same virtual origin for turbulence. The vertical displacement between these aligned profiles corresponds precisely to  $\Delta U^+$ . The virtual origin for turbulence is finally calculated as  $l_U^+ = l_T^+ - \Delta U^+$ .

## RESULTS

An overview of the simulations results is given in Figure 1, where the drag reduction is evaluated in terms of shift of the roughness function  $\Delta U^+$ . Results demonstrate the successful retrieval of drag reduction curves for all geometries, with minor discrepancies observed for sinusoidal riblets at very low  $l_g^+$  values (also visible in Figure 2). These discrepancies are likely due to insufficient resolution for such small geometries. While straight riblets achieve a  $\Delta U^+$  value around 0.8 for  $l_g^+ \approx 10$ , both considered sinusoidal geometries surpass this value. Specifically, the "LONG" geometry achieves  $\Delta U^+ \approx 1.0$ , indicating an improvement of approximately 25% compared to the straight configuration. Notably, the peaks in the drag reduction curve for sinusoidal geometries occur at larger riblet sizes, suggesting that sinusoidal riblets can extend the viscous regime to higher  $l_g^+$  values.

Further insights can be gained by examining the mean flow and turbulence virtual origins. In alignment with the earlier discussion, in Figure 2, we observe that the curves for  $l_U/h_\parallel$  and  $l_T/h_\perp$  exhibit the expected behavior: the value for  $l_U$  consistently matches the parallel protrusion height, while  $l_T$  deviates from  $h_\perp$  as the riblet size increases. As mentioned earlier we note that for the sinusoidal cases the ratio  $l_T/h_\perp$  remains constant over a broader range of  $l_g^+$  compared to straight riblets. This suggests that sinusoidal riblets may extend the viscous behavior for larger dimensions, potentially delaying the occurrence of phenomena such as Kelvin-Helmholtz instabilities and secondary motions. Future results will determine whether this

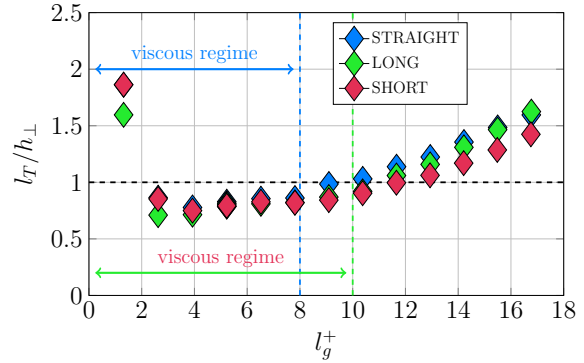
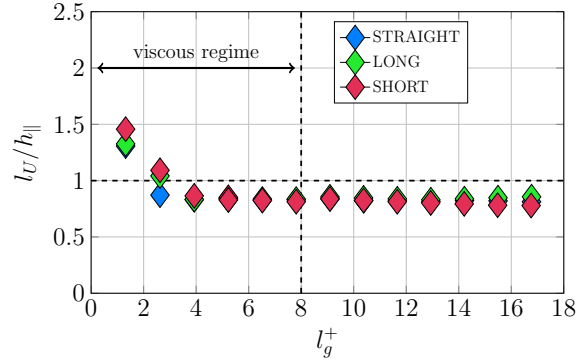


Figure 2: A comparison of virtual origins for the mean flow ( $l_U$ ) and turbulence ( $l_T$ ) to these of the longitudinal ( $h_\parallel$ ) and transverse ( $h_\perp$ ) flows, plotted as functions of the riblets size  $l_g^+$ .

behavior persists at higher Reynolds numbers and if these observations hold true for different cross-section shapes and/or different sinusoidal waves.

## REFERENCES

- [1] R. Garcia-Mayoral and J. Jiménez. Hydrodynamic stability and the breakdown of the viscous regime over riblets. *J. Fluid. Mech.*, 678:317–347, 2011.
- [2] J. I. Ibrahim, G. Gomez-de Segura, D. Chung, and R. Garcia-Mayoral. The smooth-wall-like behaviour of turbulence over drag-altering surfaces: a unifying virtual-origin framework. *Journal of Fluid Mechanics*, 915:A56, 2021.
- [3] P. Luchini. A deferred correction multigrid algorithm based on a new smoother for the Navier–Stokes equations. *Journal of Computational Physics*, 92:349–368, 1991.
- [4] P. Luchini. Reducing the turbulent skin friction. In Desideri et al., editor, *Computational Methods in Applied Sciences 1996*. Wiley, 1996.
- [5] P. Luchini, F. Manzo, and A. Pozzi. Resistance of a grooved surface to parallel flow and cross-flow. *Journal of Fluid Mechanics*, 228:87–109, 1991.
- [6] M. Quadrio and P. Ricco. Critical assessment of turbulent drag reduction through spanwise wall oscillation. *J. Fluid Mech.*, 521:251–271, 2004.